

Quantum synchronization

O.V. Zhirov⁽¹⁾ and D.L. Shepelyansky⁽²⁾⁽¹⁾Budker Institute of Nuclear Physics, 630090 Novosibirsk, Russia⁽²⁾Laboratoire de Physique Théorique, UMR 5152 du CNRS,
Université P. Sabatier, 31062 Toulouse Cedex 4, France

(Dated: July 1, 2005)

Using the methods of quantum trajectories we study numerically the phenomenon of quantum synchronization in a quantum dissipative system with periodic driving. Our results show that at small values of Planck constant \hbar the classical devil's staircase remains robust with respect to quantum fluctuations while at large \hbar values synchronization plateaus are destroyed. Quantum synchronization in our model has close similarities with Shapiro steps in Josephson junctions and it can be also realized in experiments with cold atoms.

PACS numbers: 05.45.Xt, 03.65.Yz, 74.50.+r

Since 1665, when Christiaan Huygens discovered the synchronization of two maritime pendulum clocks [1] (see [2, 3] for historical survey and modern experiments), it has been established that this universal nonlinear phenomenon appears in an abundant variety of systems ranging from clocks to reeds, cardiac pacemakers, lasers and Josephson junction (JJ) arrays [3]. Various mathematical tools have been developed to analyze synchronization in simple dissipative nonlinear models with periodic driving and complex ensembles of nonlinear coupled oscillators. Such pure mathematical concepts as Arnold tongues in the circle map [4] found their experimental implementation with Shapiro steps [5] and JJs synchronization [6]. However, till recently the treatment of synchronization has been mainly based on classical mechanics even if JJs have purely quantum origin [3, 6].

A significant progress in the theory of dissipative quantum mechanics has been done in Ref. [7]. It was further developed by various groups as reviewed in [8]. Nowadays this research line is getting more and more importance since technology goes on smaller and smaller scales where an interplay of dissipative and quantum effects becomes dominant. A typical example is given by small size JJs. Here dissipative effects are always present even if in certain cases skillful manipulations allow to realize long term coherent Rabi oscillations [9].

These reasons led to a significant number of analytical studies of quantum tunneling in presence of dissipation (see e.g. [7, 8, 10, 11, 12]). However, analytical methods have serious restrictions in a strongly nonlinear regime typical of synchronization [3]. Due to that in this paper we perform extensive numerical studies of quantum synchronization following precisely a transition from classical to quantum behavior changing effective dimensionless Planck constant \hbar by three orders of magnitude. The quantum dissipative evolution is described by the master equation for the density matrix written in the Lindblad form [13]. To perform simulations with a large number of states $N \sim 10^4$ we use the method of quantum trajectories [14, 15] which allows to reduce significantly the

number of equations compared to direct solution of the master equation (N instead of N^2). In this approach one quantum trajectory can be viewed as one individual realization of experimental run [16].

For our studies we choose a model which in the classical limit is closely related to the circle map [4] which gives a generic description of Arnold tongues and synchronization of system dynamics with an external periodic driving [3]. In absence of dissipation the evolution is described by the Hamiltonian of kicked particle fallen in a static field:

$$\hat{H} = \hat{p}^2/2 - f\hat{x} + K \cos \hat{x} \quad (1)$$

with the usual operators \hat{x} and $\hat{p} = -i\hbar \partial/\partial x$. At $f = 0$ this Hamiltonian corresponds to the kicked rotator [17], a paradigmatic model in the fields of nonlinear dynamics and quantum chaos. At non-zero f the system has been built up in experiments with cold atoms placed in laser fields and fallen in a gravitational field [18]. Non-trivial quantum effects of the static force are analyzed in [19]. Here we consider the dynamics of the model in presence of additional friction force $F = -g^2 p$. Experimentally such a force can be realized by the Doppler cooling [20]. The model can be also implemented with JJs as described in [21]. In this case effective kicks are created by an external ac-current source, f and p are proportional respectively to dc-current and voltage drop across JJ, while the friction force F naturally appears due to finite circuit resistance. The expression of K and \hbar via JJ parameters is given in [21].

The classical dynamics (1) with friction can be exactly integrated between kicks that gives a dissipative map

$$\begin{aligned} p &= (1 - g^2) p + (1 - g^2) K \sin x + f = g^2; \\ x &= x + p = g^2 + (K - g^2) \sin x + f (g^2) = g^4; \end{aligned} \quad (2)$$

where bars note new values of variables after one map iteration and $1 - g^2 = \exp(-g^2)$. Up to parameter rescaling and shifts in $x; p$, produced by static force, the map (2)

has the form of Zaslavsky map [22]. Due to contraction in p the dynamics in phase variable x is close to the circle map $x = x + K_{\text{eff}} \sin x + \beta$, [4] and demonstrates devil's staircase structure in the dependence of average momentum P on f (Fig. 1, top). Steps near rational rotation numbers $P=2$ correspond to synchronization with external periodic driving inside Arnold tongues. In average the momentum $P = f/g^2$ as it should be in an equilibrium between the external and friction forces.

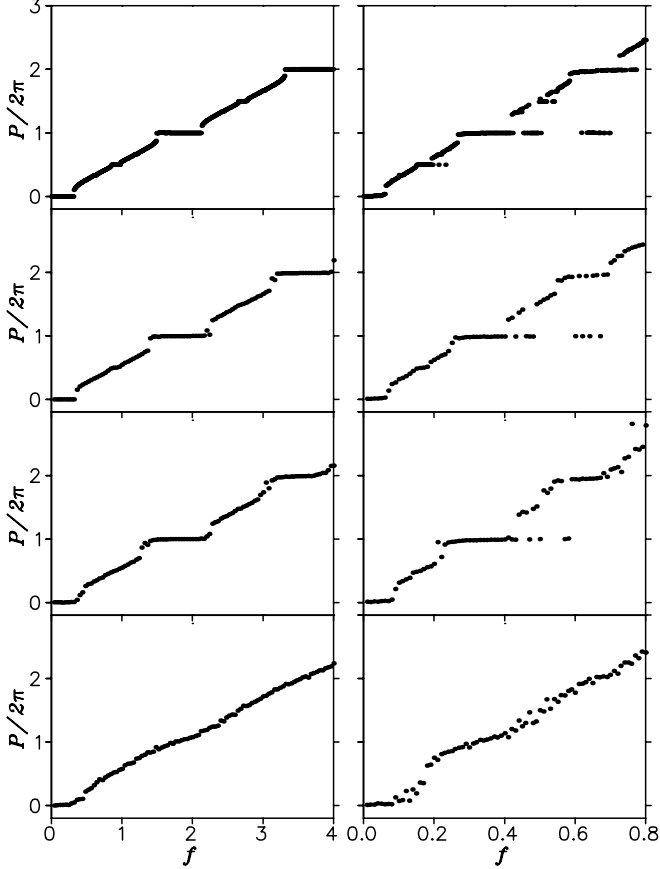


FIG. 1: Dependence of the average momentum P on static force f at $K = 0.8$ for $\gamma = 0.25$ (left column) and $\gamma = 0.05$ (right column); P is computed over $t = 500$ map iterations. From top to bottom: classical case at $\sim = 0$, $\sim = 0.012$, $\sim = 0.05$, $\sim = 0.5$. Initial conditions correspond to one classical trajectory at $x = 0$, $p = 2\pi = 0.38$ for classical dynamics. For the quantum evolution one quantum trajectory is taken at the same x, p position with the wave function in the form of minimal coherent state at given \sim .

The corresponding quantum dissipative dynamics is described by the master equation in the Lindblad form [13]:

$$\dot{\hat{\rho}} = -i[\hat{H}; \hat{\rho}] - \frac{1}{2} \sum \hat{L}^{\dagger} \hat{L} \hat{\rho} + \sum \hat{L} \hat{\rho} \hat{L}^{\dagger}; \quad (3)$$

where $\hat{\rho}$ is the density operator, f, g denotes the anticommutator, \hat{L} are the Lindblad operators, which model the effects of the environment. Following [23] we assume the

Lindblad operators in the form ($j = 1, 2$):

$$\begin{aligned} \hat{L}_1 &= g \sum_n \sqrt{\frac{P}{n+1}} |n+1\rangle \langle n| \\ \hat{L}_2 &= g \sum_n \sqrt{\frac{P}{n+1}} |n\rangle \langle n+1| \end{aligned} \quad (4)$$

These operators act on the bases of 2-periodic eigenstates of operator \hat{n} and in the regime of weak coupling and Markov approximations describe the dissipation force $F = -g^2 p$ induced by a bosonic bath at zero temperature. As in [23] the numerical simulations of quantum jumps are done for one quantum trajectory using the so-called Monte Carlo wave function approach [16]. The additional term with the constant force f is exactly integrated between jumps leading to a drift of wave function amplitudes in the space of momentum eigenstates n . The total number of states N is fixed by a condition of keeping all states with probabilities higher than 10^{-7} .

The numerical results for the quantum devil's staircase are shown in Fig. 1 for various \sim values [24]. The dependence is similar to those of $I-V$ characteristics shown in [5] with $P/V, f/I$. At small \sim values ($\sim = 0.012$) the steps remain stable with respect to quantum fluctuations. Hence, the quantum synchronization takes place inside quantum Arnold tongues. For larger $\sim = 0.05$ small steps start to disappear and at relatively large $\sim = 0.5$ the dependence $f-P$ becomes smooth so that a quantum particle slides smoothly under static force f . It is interesting to compare the cases of strong $\gamma = 0.25$ and weak $\gamma = 0.05$ dissipation (Fig. 1 left and right columns). At strong γ the contraction in p is rather rapid and the behavior is similar to the case of the circle map [4] and P grows monotonously with f . At weak γ there are many different attractors in the phase space and a classical trajectory may jump between them rather irregularly with variation of f or initial conditions. At small \sim a quantum trajectory reproduces this behavior of steps overlap rather accurately. We note that very similar structure of steps overlap is clearly seen in experimental data shown in Fig 2 of [5].

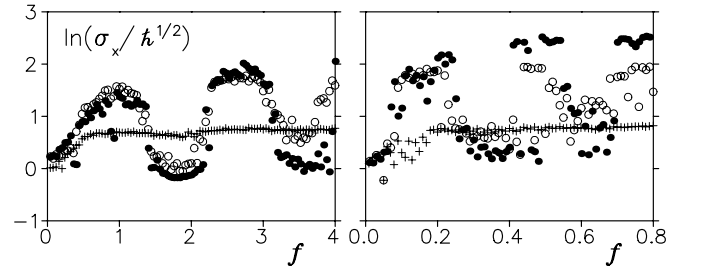


FIG. 2: Dependence of rescaled dispersion $\sigma_x \sim^{-1/2}$ of wave packet in x on force f for the cases of Fig. 1 at $\gamma = 0.25$ (left panel) and $\gamma = 0.05$ (right panel). Symbols show data at $\sim = 0.012$ (black points), $\sim = 0.05$ (open circles), $\sim = 0.5$ (+). Dispersion σ_x is averaged over $t = 500$ map iterations for one quantum trajectory with initial state of Fig. 1.

To understand the properties of dissipative quantum

dynamics we analyze the structure of wave functions associated with quantum trajectories of Fig.1. It is known that dissipation in quantum systems leads to a collapse of wave packet [25, 26, 27]. In agreement with these results and recent studies of Zaslavsky map [23] we find that the wave function in our model collapses on a compact packet of width x_p (dispersion) in coordinate and momentum respectively (e.g. $|j(x)| \sim \exp(-x^2/(4x_p^2))$) [28]. The width x_p depends nontrivially on f as it is shown in Fig.2. Inside the steps with synchronization the value of x_p is strongly reduced while in the sliding regime between steps its value is significantly enhanced. In the limit of small \hbar where quantum synchronization takes place the rescaled width $x_p = \tilde{x}_p$ shows approximately the same functional dependence on f for all \hbar . This functional dependence on f is completely changed at large \hbar where synchronization is absent and where x_p is not very sensitive to f . For small \hbar (Fig.2 right) the dependence on f becomes more irregular in agreement with more complicated step structure seen in Fig.1 (right). We note that at the same time p_p remains practically insensitive to variation of f (data not shown). This is related to the fact that in momentum p the dynamics is close to a simple contraction while in coordinate x the nonlinear dynamics significantly depends on the system parameters (see discussion below).

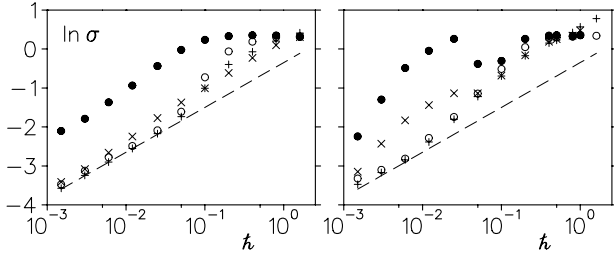


FIG. 3: Dependence of dispersion in x (x_p) and p (p_p) on f for $K = 0.8$ at $\hbar = 0.25$ (left) and $\hbar = 0.05$ (right); \tilde{x}_p is averaged over $t = 5000$ map iterations. Left panel: $f = 1.1$ (points for x and for p), $f = 1.9$ (open circles for x and + for p). Right panel: $f = 0.21$ (points for x and for p), $f = 0.37$ (open circles for x and + for p). Dashed line shows the dependence $\tilde{x}_p = (\sim 2)^{-1/2}$. Initial state is as in Fig.1.

To check more accurately the scaling $x_p; p_p / \hbar \sim \tilde{x}_p$ we choose two values of force f and vary \hbar by three orders of magnitude (see Fig.3). One value of f is taken on a synchronization plateau when a classical attractor is a fixed point in the phase space and another is taken on a slope when the classical dynamics has attractor in a form of invariant curve as it is shown in Fig.4 for $\hbar = 0.25$. Clearly x_p is significantly larger in the case of invariant curve than in the case of fixed point. Intuitively it is rather natural since in the first case variation of phase x is unbounded in 2π while in the later case the phase value is fixed (Fig.4). Thus we may conclude that quantum synchronization gives a significant reduction of quantum fluctuations. At the same time fluctuations in p charac-

terized by p_p are not sensitive to the choice of f . In the limit of small \hbar the numerical data of Fig.3 clearly show that the wave packet dispersion scales as

$$x_p \sim \hbar^{1/2} / \tilde{x}_p : \quad (5)$$

In the synchronization regime the dispersion is even close to its minimum value with $x_p = \hbar^{1/2} / \tilde{x}_p = \sim 2$ (dashed line in Fig.3). At smaller dissipation the asymptotic dependence $\tilde{x}_p / \hbar^{1/2}$ starts at smaller values of \hbar (cf. left and right panels of Fig.3). Indeed, the wave packet width grows dispersively during time $t = t_p$ that makes \tilde{x}_p larger at small \hbar . The dependence (5) is in agreement with the data obtained in the regime of wave packet collapse in [23] for a smaller range of \hbar variation (note also [28]).

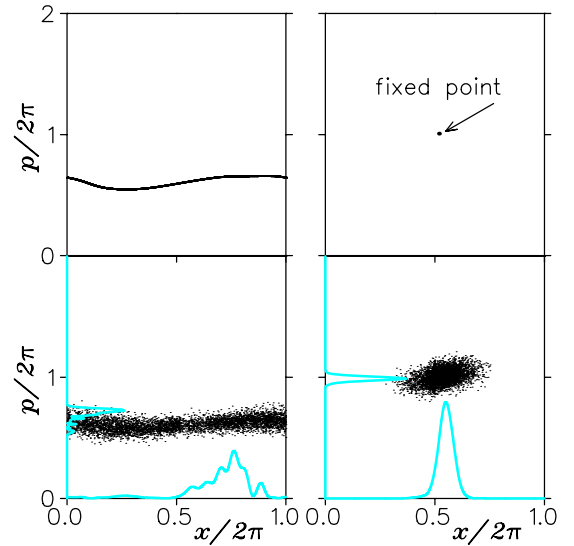


FIG. 4: (Color online) Poincaré section for $K = 0.8$, $\hbar = 0.25$ at $f = 1.1$ (left) and $f = 1.9$ (right). Top: classical case; bottom: quantum case at $\hbar = 0.05$, points mark the average $x; p$ positions of wave packet; light blue (gray) curves on $x; p$ axes show at $t = 5000$ the quantum probability distribution in x and p respectively (arbitrary units). Number of map iterations $t = 5000$, initial state is as in Fig.1.

Other properties of quantum dissipative dynamics can be understood from Poincaré phase space plots. In the classical case two typical examples are shown in Fig.4 (top) with invariant curve and fixed point attractors. In the corresponding quantum case we plot in the phase space the values of x, p averaged over a wave function of a given quantum trajectory at each map iteration (integer time t) (Fig.4 bottom, quantum probability distributions are also shown). The quantum Poincaré plot reproduces correctly the global structure of classical phase space but additional noise produced by quantum fluctuations is clearly visible. This quantum noise creates an effective width of an invariant curve and replaces a fixed point by a spot of finite size. The size of these fluctuations is approximately given by x_p and p_p . They decrease with \hbar according to the relation (5). Due to this quantum noise two quantum trajectories with the same initial

state can drop on different attractors and thus contribute to different plateaus in the devil's staircase (Fig.1). We indeed observed such cases simulating different quantum trajectories with the same initial state (data not shown). However, convergence to different plateaus takes place only at relatively weak dissipation ($\gamma = 0.05$) when there are many different classical attractors close in a phase space and quantum noise may give transitions between them. At strong dissipation ($\gamma = 0.25$) the attractors are well separated and different quantum trajectories converge to the same plateau.

The above results show that the quantum synchronization has close links with the classical synchronization in presence of noise. The latter has been intensively investigated and it is known that the synchronization plateaus are preserved if the noise amplitude is significantly smaller than their size [3]. In a similar way we may conclude that the quantum synchronization remains robust with respect to quantum fluctuations until their amplitude (proportional to $\sqrt{\hbar}$) remains smaller than the size of a synchronization plateau. We also checked that the classical dynamics (2) with additional noise in $x; p$, with dispersion values $\sigma_x; \sigma_p$ taken from the quantum evolution, gives the dependence P vs. \hbar which is close to the quantum result (data not shown).

Above we discussed quantum synchronization with external periodic driving. It would be interesting to investigate the synchronization of two quantum nonlinear pendulum clocks to have a quantum version of the Huygens experiment [1]. Recently, first numerical simulations in such kind of regime (two quantum coupled Duffing oscillators) has been performed in [29]. Their results show that in the case when the quasi-integrable dynamics of oscillators becomes synchronized (entrained) the von Neumann entropy of one oscillator drops significantly. This result is in a qualitative agreement with our data showing that the dispersion of quantum state drops significantly on synchronization plateaus (Fig. 2) [30]. Further investigations of quantum synchronization in coupled nonlinear systems are of great interest. For example, quantization may produce nontrivial effects in the synchronization transition in a disordered JJ series array discussed in [31].

Modern technological progress allows to study the regime of quantum synchronization with small size JJs (e.g. similar to those of [9]) or with cold or BEC atoms (e.g. like in [18]). This should open new perspectives for synchronization of quantum objects with possible applications to quantum computations.

This work was supported in part by the EC IST-FET projects EDIQU, EuroSQIP and (for OVZ) by RAS Joint scientific program "Nonlinear dynamics and solitons".

- [1] C. Huygens, *uvres complètes*, vol. 15, Swets & Zeitlinger B.V., Amsterdam (1967).
- [2] M. Bennett, M.F. Schatz, H. Rockwood and K. Wiesenfeld, *Proc. R. Soc. Lond. A* 458, 563 (2002).
- [3] A. Pikovsky, M. Rosenblum and J. Kurths, *Synchronization: a universal concept in nonlinear sciences*, Cambridge University Press, Cambridge UK (2001).
- [4] V.I. Arnold, *Izv. Akad. Nauk SSSR Ser. Mat.* 25 (1), 21 (1961) [*AMS Transl. Ser. 2*, 28, 61 (1963)].
- [5] S. Shapiro, *Phys. Rev. Lett.* 11, 80 (1963).
- [6] A.K. Jain, K.K. Likharev, J.E. Lukens and J.E. Sauvageau, *Phys. Rep.* 109, 309 (1984).
- [7] A.O. Caldeira and A.J. Leggett, *Phys. Rev. Lett.* 46, 211 (1981); *Ann. Phys. (N.Y.)* 149, 374 (1983).
- [8] U. Weiss, *Quantum dissipative systems*, World Sci., Singapore (1999).
- [9] D. Vion, A. Aassime, A. Cottet, P. Joyez, H. Pothier, C. Urbina, D. Esteve and M.H. Devoret, *Science* 296, 886 (2002).
- [10] A.J. Leggett, S. Chakravarty, A.T. Dorsey, M.P.A. Fisher, A. Garg and W. Zwerger, *Rev. Mod. Phys.* 59, 1 (1987).
- [11] Y.N. Ovchinnikov and B.I. Ivlev, *Phys. Rev. B* 39, 9000 (1989).
- [12] D.V. Averin and A.A. Odintsov, *Sov. J. Low Temp. Phys.* 16, 7 (1990); 16, 725 (1990).
- [13] G. Lindblad, *Commun. Math. Phys.* 48, 119 (1976).
- [14] T.A. Brun, I.C. Percival, and R. Schack, *J. Phys. A* 29, 2077 (1996).
- [15] T.A. Brun, *Am. J. Phys.* 70, 719 (2002).
- [16] J. Dalibard, Y. Castin, and K.M. Mølmer, *Phys. Rev. Lett.* 68, 580 (1992).
- [17] F.M. Izrailev, *Phys. Rep.* 196, 299 (1990).
- [18] Z.-Y. Ma, M.B. d'Ary and S.A. Gardiner, *Phys. Rev. Lett.* 93, 164101 (2004).
- [19] S.W. Imberger, I. Guameri and S. Fishman, *Phys. Rev. Lett.* 92, 084102 (2004).
- [20] M.O. Scully and M.S. Zubairy *Quantum Optics* Cambridge University Press, Cambridge UK (1997).
- [21] R. Graham, M. Schlautmann and D.L. Shepelyansky, *Phys. Rev. Lett.* 67, 255 (1991).
- [22] G.M. Zaslavsky, *Phys. Lett. A* 69, 145 (1978).
- [23] G. Carib, G. Benenti and D.L. Shepelyansky, quant-ph/0503188.
- [24] We show here data for one typical case at $K = 0.8$, similar results have been seen in the range $0.4 < K < 2$ with quasi-integrable dynamics.
- [25] I.C. Percival, *J. Phys. A* 27, 1003 (1994).
- [26] J. Halliwell and A. Zoupas, *Phys. Rev. D* 52, 7294 (1995).
- [27] R. Schack, T.A. Brun, and I.C. Percival, *J. Phys. A* 28, 5401 (1995).
- [28] We study here the nonlinear dynamics in a quasi-integrable regime without Ehrenfest explosion [23].
- [29] M.J. Everitt, T.D. Clark, P.B. Stiel, J.F. Ralph, A.R. Bulsara and C.J. Harland, *New J. Phys.* 7, 64 (2005).
- [30] Let us note that a large value of entropy found in [29] in the chaotic regime at small \hbar should be related to the Ehrenfest explosion discussed in [23].
- [31] K. Wiesenfeld, P. Colet and S.H. Strogatz, *Phys. Rev. Lett.* 76, 404 (1996).